Computational study on the kinetics of the reaction between Ca2+ and Urea

Alvaro Cimas, Jose A. Gamez, Otilia Mó, Manuel Yáñez, Jean-Yves Salpin

Computational study on the kinetics of the reaction between Ca^{2+} and Urea

Alvaro Cimas*, José A. Gámez, Otilia Mó and Manuel Yáñez

Departamento de Química C-IX, Universidad Autónoma de Madrid, Cantoblanco, 28049-Madrid, Spain.

and

Jean-Yves Salpin

Université d'Evry Val d'Essonne, Laboratoire Analyse et Modélisation pour la Biologie et l'Environnement, Université d'Evry Val d'Essonne, CNRS UMR 8587, Bâtiment Maupertuis, Boulevard François Mitterrand, 91025 Evry Cedex, France.

*corresponding author : alvaro.cimas@uam.es
FAX No. +34-91-4975238

Abstract

A computational study, in the framework of statistical kinetic theories, of the reaction of Ca^{2+} with urea has been carried out. The kinetically preferred products are NH_3 + $[CaOCNH]^{2+}$, which are the fifth products in order of stability. The second kinetically preferred products are $[CaNH_2^+]$ + $[NH_2CO]^+$, followed by $[CaNH_3]^{2+}$ + HNCO, whereas the most stable ones, NH_4^+ + $[CaNCO]^+$ and NH_4^+ + $[CaOCN]^+$, appear only in residual quantities. These estimates are in agreement with the experimental evidence and provide a suitable mechanism to understand the competition between Coulomb explosion and neutral loss processes.

1. Introduction

Doubly or multiply charged species are rare in the gas phase, even nowadays when the advent of electrospray ionization techniques made possible to generate them in the gas-phase from aqueous solution [1]. This is so because most of these species are either thermodynamically or kinetically unstable [2]. This is indeed the case when doubly charged molecular ions are formed by association of a neutral base with a doubly-charged transition metal ion, and although species like $Cu(H_2O)^{2+}$, $Cu(NH_3)^{2+}$ or $Pb(H_2O)^{2+}$, have been detected in the gas phase [3-5], and their lifetimes have been predicted to be extremely large when they are in the lower vibrational states [6], in most cases, when a transition metal dication, M^{2+}, is attached to an organic base, B, the system undergoes an spontaneous deprotonation process and only the $[(B\text{-}H)M]^+$ monocation is experimentally observed [7-9]. It has been argued that this behavior is related with the usually high recombination energy of these doubly-charged metal ions, which, leads

accordingly to an oxidation of the base and to its subsequent deprotonation [10]. This is not the case for alkaline-earth dications, in particular for Ca^{2+}, whose recombination energy (12.0 eV [11]) is sizably smaller than that of Cu^{2+} (20.3 eV) or Ni^{2+} (18.2 eV)[11], for instance. The main consequence is that the association of Ca^{2+} to a base, B, may not be followed by a deprotonation process and therefore the corresponding $[BCa]^{2+}$ doubly-charged species can be detected and isolated in the gas phase. This opened the possibility of studying for the first time the unimolecular reactivity of complexes formed by this metal dication with different neutrals, namely urea, glycine, thiourea and selenourea [12-15]. One of the most interesting conclusions of these studies is that in general there are two types of processes which compete, typical Coulomb explosions, in which the doubly-charged complex yields two monocations, and neutral loss fragmentations which produced a new doubly-charged species of smaller mass. Interestingly for instance, in both the reactions of Ca^{2+} with urea and thiourea evidences of formation of $[CaNH_3]^{2+}$ complexes have been reported in the literature [12,14]. Although some clues about the mechanisms in which these products are formed can be extracted from the topology of the potential energy surface, this constitutes only a first rough approach, because, quite often the products which are thermodynamically favored are not kinetically favored. This is likely the case for Ca^{2+} + urea reactions in the gas phase, where some of the products generated through Coulomb explosions are among the most stable, whereas experimentally they are not the most abundant [12]. The aim of this paper is precisely to carry out a study of the kinetic of this reaction, in order to offer a rationale of the observed products distribution.

2. Computational details

The potential energy surface (PES) of the urea-Ca^{2+} reaction was obtained[12] through the use of standard density functional theory calculations on neutral urea (U) and on $[Ca(U)]^{2+}$ complexes, using the Gaussian 98 package of programs [16]. Optimized geometries and vibrational frequencies were obtained with the B3LYP exchange-correlation functional [17,18] and with the cc-pWCVTZ basis sets [19]. The same theoretical scheme was used to obtain structural and energetic information about other stationary points of the $[Ca(U)]^{2+}$ potential energy surface (PES). To facilitate the discussion which follows we have plotted in Figure 1 a simplified energy profile of this complicated PES, which has been fully described in ref. [12].

Based on the characteristics of this energy profile we have developed the mechanistic model shown in Scheme 1 for the reaction between urea and Ca^{2+}, where the B3LYP/cc-pWCVTZ relative energies (in kcal/mol) are provided for the relevant intermediates and final products of the reaction. Details about geometrical parameters and relative energies of all species involved in the reaction can be found in our previous work [12].

Due to the complexity of the reaction characterized by a large number of intermediates [12], the kinetic calculations have been carried out in the framework of the statistical kinetic theories. Such an approach, despite its intrinsic limitations [20], basically provides the unique tool for addressing at a semi-quantitative level, mechanistically complicated reactions as the present one.

For the kinetic calculations concerning the formation of the initial intermediate **1** (k_{capt}), as well as for those processes where no transition structure, i.e., first-order saddle

point, was found (i.e., the dissociations corresponding to k_{4e}, k_{5d}, k_{5e}, k_{6e}, k_{8d} and k_{8f}) we adopted the microcanonical variational transition state theory (μVTST) in its vibrator formulation [21,22]. More specifically, the potential energy paths of the above processes were first scanned. Subsequently, at each point of the scan, the Hessian matrices describing the modes orthogonal to the reaction path were evaluated according to the standard procedure of Miller et al. [23].

For the unimolecular reactions involving all the intermediates, the microcanonical rate coefficients have been calculated employing the following usual equation of RRKM theory [24]:

$$k(E,J) = \sigma N^{\#}(E,J)/[h\rho(E,J)] \quad (1)$$

where σ is the reaction symmetry factor, $N^{\#}(E,J)$ is the number of the states of the transition state and $\rho(E,J)$ is the density of the states at the minimum.

The determination of the density and sum of states were calculated through the Forst algorithm [25] using the corresponding frequencies and moments of inertia (the data for intermediates and transition states are provided in Tables 1 and 2, respectively). The possibility of tunneling was accounted for in terms of a monodimensional probability according to the generalized Eckart potential [26]. All the kinetic calculations were carried out with our own routines.

3. Results and discussion

The gas-phase reaction of urea with Ca^{2+} proceeds via a typical addition–elimination mechanism [12]. As illustrated in Figure 1, initially the intermediate **1** is formed from the reactants without involving any transition state. In addition to fragmentations into final products, **1** may evolve to other intermediates through migration of Ca^{2+} accompanied by the rotation of one of the amino groups (**2**) or the 1,3-H shift from one of the amino group to the other (**4**). **2**, which can also be formed directly from the reactants, can lead to a relevant intermediate, **6**, through the 1,3-H shift between the two amino groups, or undergo a Coulomb explosion. **4** can isomerize by migration of the ammonia molecule attached to the carbon atom to calcium to yield a very stable intermediate (**5**) or through an inversion of the imino group leading to the intermediate **6**. **6** can either undergo two different Coulomb explosions or evolve through isomerization to **7** and, finally, **7** can isomerize to **8** through migration of the ammonia group from the carbon to the calcium atom. In any case the most stable intermediate is **1**. There are seven possible exothermic products for this reaction, namely, NH_4^+ + $[CaOCN]^+$, NH_4^+ + $[CaNCO]^+$, $[CaNH_2^+]$ + $[NH_2CO]^+$, $[CaNH_3]^{2+}$ + HNCO, NH_3 + $[CaOCNH]^{2+}$, NH_3 + $[OCNHCa]^{2+}$, and, CaO^+ + $[H_2NCNH_2]^+$, in order of decreasing exothermicity. Therefore, it seems that, from the thermodynamic point of view, NH_4^+ elimination seems to be favored over elimination of ammonia. As can be seen, some of the processes depicted in (Figure 1) do not involve any transition structure. As already mentioned, this is the case for the initial capture process, but also for all fragmentations in which a molecule of ammonia is lost: **4** $\rightarrow$ NH_3 + $[CaOCNH]^{2+}$, **5** $\rightarrow$ NH_3 + $[CaOCNH]^{2+}$, **6** $\rightarrow$ NH_3 + $[CaOCNH]^{2+}$, **8** $\rightarrow$ NH_3 + $[OCNHCa]^{2+}$. Therefore in the treatment of k_{4e}, k_{5e}, k_{6e} and k_{8f}, the loose transition state approach was employed.

On the basis of Scheme 1, the steady-state solution of the master equation leads to the microcanonical expression (2) of the overall rate coefficient:

$$k_{overall} = k_a + k_b + k_c + k_d + k_e + k_f + k_g \tag{2}$$

, where the individual coefficients for the different channels (a: NH_4^+ + $[CaNCO]^+$, b: NH_4^+ + $[CaOCN]^+$, c: $[CaNH_2^+]$ + $[NH_2CO]^+$, d: $[CaNH_3]^{2+}$ + HNCO, e: NH_3 + $[CaOCNH]^{2+}$, f: NH_3 + $[OCNHCa]^{2+}$, g: CaO^+ + $[H_2NCNH_2]^+$) are given by the following formulas:

$$k_a = \frac{k_{6a}}{C}\left[k_{26}GI + k_{46}\left(k_{14}\frac{I}{E} + k_{26}\,k_{-46}\frac{GI}{CE}\right)\right] \tag{3}$$

$$k_b = \frac{k_{6b}}{C}\left[k_{26}GI + k_{46}\left(k_{14}\frac{I}{E} + k_{26}\,k_{-46}\frac{GI}{CE}\right)\right] \tag{4}$$

$$k_c = k_{2c}\,GI \tag{5}$$

$$k_d = k_{5d}\,D\left(k_{14}\frac{I}{E} + k_{26}\,k_{-46}\frac{GI}{CE}\right) + \frac{k_{8d}\,AB}{C}\left[k_{26}GI + k_{46}\left(k_{14}\frac{I}{E} + k_{26}\,k_{-46}\frac{GI}{CE}\right)\right] \tag{6}$$

$$k_e = \left(k_{4e} + k_{5e}\,D + \frac{k_{6e}\,k_{46}}{C}\right)\left[k_{26}GI + k_{46}\left(k_{14}\frac{I}{E} + k_{26}\,k_{-46}\frac{GI}{CE}\right)\right] + \frac{k_{6e}k_{26}GI}{C} \tag{7}$$

$$k_f = \frac{k_{8f}\,AB}{C}\left[k_{26}GI + k_{46}\left(k_{14}\frac{I}{E} + k_{26}\,k_{-46}\frac{GI}{CE}\right)\right] \tag{8}$$

$$k_g = k_{1g}\, I \tag{9}$$

, where:

$$A = \frac{k_{78}}{k_{-78} + k_{8d} + k_{8f}} \tag{10}$$

$$B = \frac{k_{67}}{k_{-67} + k_{78} - k_{78} A} \tag{11}$$

$$C = k_{-26} + k_{-46} + k_{67} + k_{6a} + k_{6b} + k_{6e} - k_{-67} B \tag{12}$$

$$D = \frac{k_{45}}{k_{-45} + k_{5d} + k_{5e}} \tag{13}$$

$$E = k_{-14} + k_{45} + k_{46} + k_{4e} - k_{-45} D - \frac{k_{46}\, k_{-46}}{C} \tag{14}$$

$$F = k_{-12} + k_{26} + k_{2c} - \frac{k_{-26}\, k_{26}}{C} - \frac{k_{26}\, k_{-26}\, k_{46}\, k_{-46}}{C^2 E} \tag{15}$$

$$G = \frac{k_{12}}{F} + \frac{k_{14}\, k_{-26}\, k_{46}}{CEF} \tag{16}$$

$$H = k_{-capt} + k_{12} + k_{14} + k_{1g} - \frac{k_{14}\, k_{-14}}{E} - \frac{k_{-14}\, k_{26}\, k_{-46}\, G}{CE} - k_{-12}\, G \tag{17}$$

$$I = \frac{k_{capt}}{H} \tag{18}$$

The above expressions were subsequently thermally averaged, according to Boltzmann distribution, in order to obtain the final canonical rate coefficients.

In Fig. 2 the overall and individual (for the different channels) canonical rate coefficients are plotted against the temperature. A typical Arrhenius behavior is observed for the overall reaction coefficient, with only small deviations from linearity at large temperatures. The computed overall rate coefficient at 300 K in vacuum is 6.3×10^{-20} cm^3 s^{-1} $molecule^{-1}$.

Individual rate coefficients follow also similar patterns, but the most interesting features concern their relative values. It is readily seen in Fig. 2 that the canonical rate constants for the different channels can be ordered in magnitude, at 300 K, as follows: $k_e > k_c > k_d > k_b > k_a > k_f > k_g$. These values lead to reaction product branching ratios which are shown at different temperatures in Table 3. The present calculations, at 300 K, predict the major product (about 58 %) to be NH_3 + $[CaOCNH]^{2+}$, which are the fifth products in stability order, followed by $[CaNH_2^+]$ + $[NH_2CO]^+$ (23 %) and $[CaNH_3^{2+}]$ + HNCO (17 %) whereas only residual quantities of NH_4^+ + $[CaOCN]^+$ and NH_4^+ + $[CaNCO]^+$ should be produced. This is interesting since, under kinetic control, it is predicted that the preferred product is less exothermic (-87.6 kcal/mol at the B3LYP level) than the most stable products which are produced only to a very small extent. This result is perfectly consistent with the experimental observations [12] which showed that the most abundant product was NH_3 + $[CaOCNH]^{2+}$ at low center of mass (E_{cm}) collision energies. Its abundance is about three times (2.60) that of $[CaNH_2^+]$ + $[NH_2CO]^+$ at E_{cm}= 4.38 eV (that is 10 eV in the laboratory frame, N_2 being used as collision gas), in very good agreement with our calculated branching ratios (0.23/0.58 = 2.52). Furthermore, our data well

predict the inversion of the branching ratio for these two reactions. It occurs in the vicinity of 350 K and experimentally for E_{cm}=5.25 eV (E_{lab}=12 eV). From this study, it also turns out that the very small abundance of ammonium ions onto MS/MS spectra could be also due to kinetic considerations. In summary, we can conclude that the calculated PES for this reaction provides mechanisms which match the experimentally observed products distribution. Also interestingly, although the energy barrier associated with Coulomb explosions are similar or even lower than those associated with neutral losses, they are, at least in the present case, less favorable from the kinetic viewpoint. Hence, although some of the monocations produced in some of these Coulomb explosions are the most stable products from a thermodynamic point of view, they are not among the most abundant ones.

4. Conclusions

We have carried out a computational study on the kinetics of the reaction of urea with calcium. The computed overall rate coefficient at 300 K is about 6.3×10^{-20} cm^3 s^{-1} $molecule^{-1}$. The most important conclusion of our work is that the kinetically preferred product (accounting for almost three fifths of products) is NH_3 + $[CaOCNH]^{2+}$, that are not the most favoured products from the thermodynamical point of view. The most stable products, NH_4^+ + $[CaOCN]^+$ and NH_4^+ + $[CaNCO]^+$, are only found as a residual products, whereas the kinetic calculations show that $[CaNH_2^+]$ + $[NH_2CO]^+$ are the second most favored products (with branching ratios nearly 0.23) and this reaction channel becomes predominant at high temperatures. Finally, this study shows that, at 300 K, elimination of ammonia is preferred over formation of NH_4^+. These estimates are in

agreement with the experimental evidence and provide suitable mechanisms to understand the competition between Coulomb explosion and neutral loss processes.

Acknowledgements. This work has been partially supported by the DGI Project No. BQU2003-00894, and by the Project MADRISOLAR, Ref.: S-0505/PPQ/0225 of the Comunidad Autónoma de Madrid. AC acknowledges a postdoctoral contract associated to the Project MADRISOLAR. A generous allocation of computing time at the CCC of the UAM is also acknowledged.

Reference

[1] P. Jayaweera, A. T. Blades, M. G. Ikonomou, P. Kebarle, J. Am. Chem. Soc. 112 (1990) 2452.

[2] D. Schröder, H. Schwarz, J. Phys. Chem. A 103 (1999) 7385.

[3] D. Schröder, H. Schwarz, J. Wu, C. Wesdemiotis, Chem. Phys. Lett. 343 (2001) 258.

[4] T. J. Shi, G. Orlova, J. Z. Guo, D. K. Bohme, A. C. Hopkinson, K. W. M. Siu, J. Am. Chem. Soc. 126 (2004) 7975.

[5] T. J. Shi, J. F. Zhao, A. C. Hopkinson, K. W. M. Siu, J. Phys. Chem. B 109 (2005) 10590.

[6] A. Palacios, I. Corral, O. Mó, F. Martín, M. Yáñez, J. Chem. Phys. 123 (2005) 014315 (1.

[7] S. Guillaumont, J. Tortajada, J.-Y. Salpin, A. M. Lamsabhi, Int. J. Mass Spectrom. 243 (2005) 279.

[8] N. G. Tsierkezos, D. Schroder, H. Schwarz, Int. J. Mass Spectrom. 235 (2004) 33.

[9] A. M. Lamsabhi, M. Alcamí, O. Mó, M. Yáñez, J. Tortajada, J. Y. Salpin, ChemPhysChem 8 (2007) 181.

[10] A. M. Lamsabhi, M. Alcamí, O. Mó, M. Yáñez, J. Tortajada, J. Phys. Chem. A 110 (2006) 1943.

[11] NIST Chemistry Webbook. Standard Reference Database Number 69. Eds. P.J. Linstrom and W.G. Mallard, Release June 2005, National Institute of Standards and Technology, Gaithersburg MD, 20899 (http://webbook.nst.gov). (2005).

[12] I. Corral, O. Mó, M. Yáñez, J.-Y. Salpin, J. Tortajada, L. Radom, J. Phys. Chem. A 108 (2004) 10080.

[13] I. Corral, et al, Chem. Eur. J 12 (2006) 6787.

[14] C. Trujillo, O. Mó, M. Yáñez, J. Y. Salpin, J. Tortajada, ChemPhysChem 8 (2007) 1330.

[15] C. Trujillo, O. Mó, M. Yáñez, J. Tortajada, J.-Y. Salpin, J. Phys. Chem. B in press (2008).

[16] M. J. Frisch, et al, Gaussian98. Gaussian, Inc., Pittsburgh PA, 1999.

[17] A. D. Becke, J. Chem. Phys. 98 (1993) 1372.

[18] C. Lee, W. Yang, R. G. Parr, Phys. Rev. B 37 (1988) 785.

[19] M. A. Iron, M. Oren, J. M. L. Martin, Mol. Phys. 101 (2003) 1345.

[20] T. Baer, W. L. Hase, Unimolecular Reaction Dynamics Theory and Experiments, Oxford University Press, Oxford, 1996.

[21] B. C. Garrett, D. G. Truhlar, J. Chem. Phys. 70 (1979) 1593.

[22] X. Hu, W. L. Hase, J. Chem. Phys. 95 (1991) 8073.

[23] W. H. Miller, N. C. Handy, J. E. Adams, J. Chem. Phys. 72 (1980) 99.

[24] P. J. Robinson, K. A. Holbrook, Unimolecular Reactions, Wiley, New York, 1972.

[25] W. Forst, Theory of Unimolecular Reactions, Academic Press, New York, 1973.

[26] W. H. Miller, J. Am. Chem. Soc. 101 (1979) 6810.

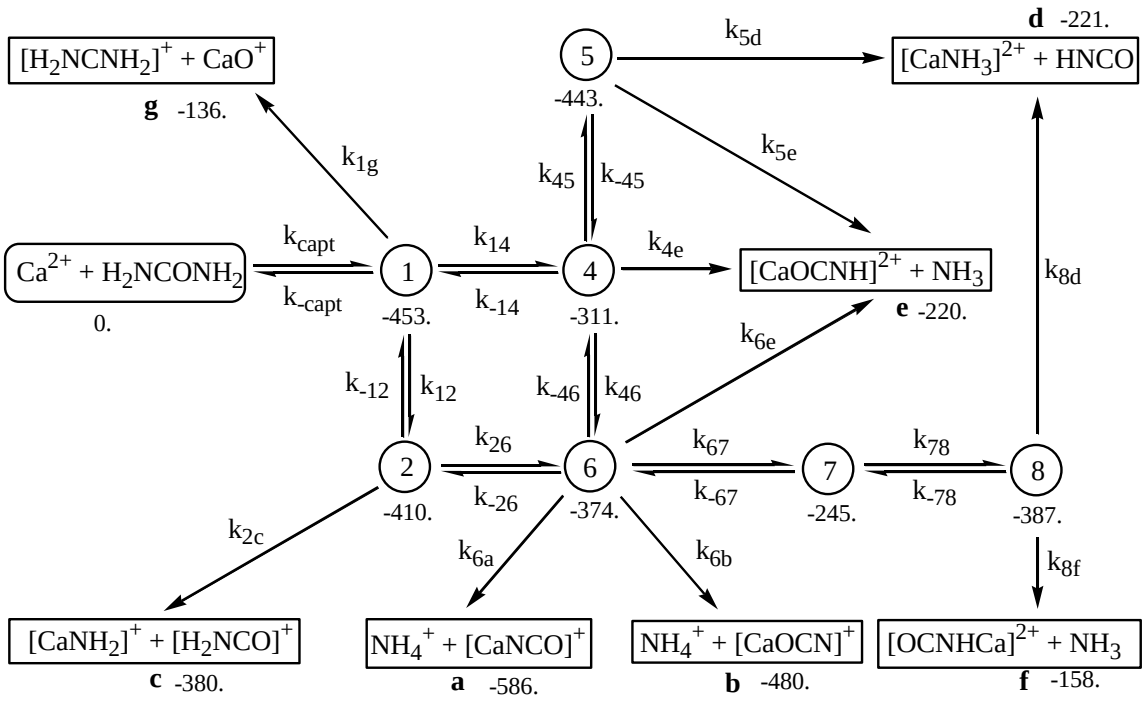

Scheme 1. Mechanistic model for the kinetic study employed in the present work (relative energies at 0 K are in kJ/mol).

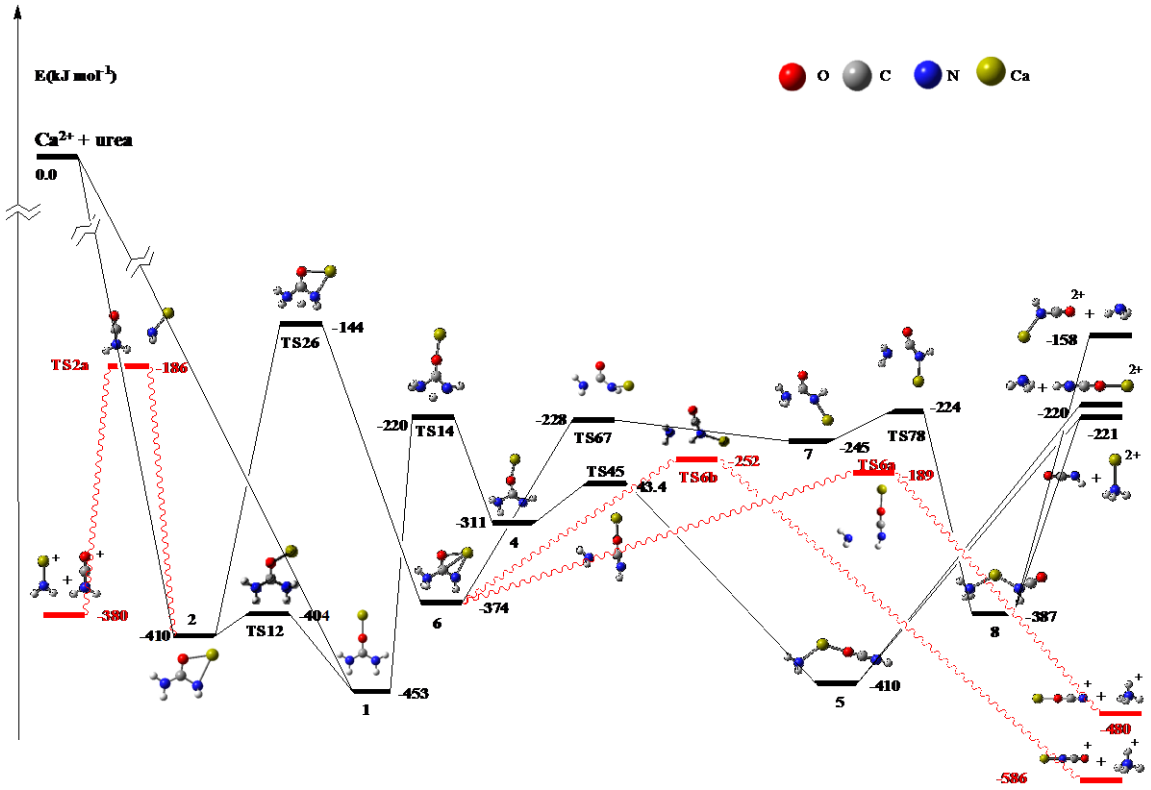

Fig. 1. Simplified energy profile of urea + Ca^{2+} reactions. Values taken from ref. [12]. Red wavy lines correspond to coulomb explosions.

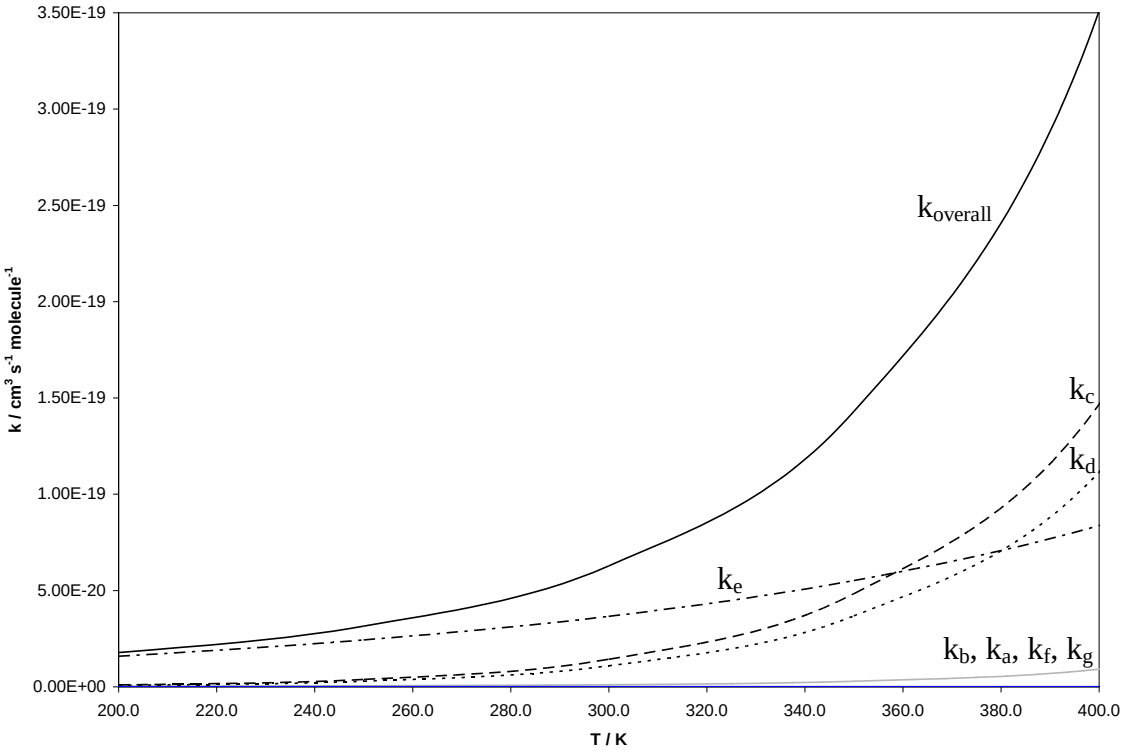

Fig. 2. Overall and individual rate coefficients (cm^3 s^{-1} $molecule^{-1}$) plotted versus the temperature (K).

Table 1. Vibrational frequencies (cm^{-1}) and rotational constants (GHz) for the different intermediates located on the $[CaU]^{2+}$ potential energy surface. The notation is the same as employed in [1].

	1	**2**	**4**	**5**	**6**	**7**	**8**
Vibrational	122	39	132	28	14	68	16
frequencies	123	203	140	31	138	86	43
	341	341	160	101	234	144	53
	358	421	326	102	326	319	117
	464	511	505	297	462	439	297
	507	585	573	315	612	515	355
	559	673	581	317	620	527	424
	565	675	757	360	734	719	595
	641	741	878	590	842	724	597
	761	883	1044	592	1016	983	622
	1049	1048	1079	600	1063	995	632
	1062	1120	1080	600	1159	1238	1209
	1129	1203	1240	1333	1376	1434	1276
	1563	1435	1484	1370	1491	1447	1375
	1570	1598	1629	1660	1620	1625	1660
	1682	1629	1646	1661	1639	1654	1660
	1700	1741	1802	2472	1724	1904	2349
	3557	3414	3364	3398	3343	3322	3393
	3574	3468	3445	3466	3422	3369	3428
	3681	3500	3455	3467	3423	3452	3460
	3684	3617	3536	3707	3559	3482	3462
A	10.4	10.3	10.2	12.9	11.3	9.5	16.2
B	1.6	2.1	1.5	1.1	2.1	1.4	1.1
C	1.4	1.8	1.3	1.0	1.8	1.3	1.0

Table 2. Vibrational frequencies (cm^{-1}) and rotational constants (GHz) for the different relevant transition states located on the $[CaU]^{2+}$ potential energy surface. The notation is the same as employed in [1].

	TS12	**TS14**	**TS26**	**TS45**	**TS46**	**TS67**	**TS78**	**TS1a**	**TS2a**	**TS6a**	**TS6b**
Vibrational	138i	1790i	1941i	117i	784i	330i	234i	37i	62i	195i	114i
frequencies	117	113	144	79	78	60	64	30	17	58	42
	369	132	227	103	99	131	112	71	34	86	88
	431	345	296	104	137	175	154	78	107	134	103
	505	382	318	198	311	333	324	80	205	188	133
	606	511	510	362	456	458	342	388	317	328	251
	629	587	566	381	520	475	492	490	377	407	304
	669	785	686	403	536	612	565	644	498	433	363
	750	828	749	473	582	703	646	673	499	531	378
	884	955	960	484	693	957	682	703	585	589	437
	972	1026	973	528	963	976	734	713	603	680	562
	1097	1157	1009	609	981	1144	1205	1062	608	1158	592
	1176	1185	1151	1219	1169	1287	1307	1111	1101	1245	1211
	1482	1323	1295	1300	1427	1437	1361	1224	1218	1281	1329
	1593	1352	1422	1673	1636	1628	1647	1592	1535	1670	1682
	1652	1604	1600	1675	1646	1641	1666	1620	1550	1672	1683
	1717	1726	1697	2339	1979	1914	2162	1822	2406	2319	2459
	3468	2087	1945	3440	3388	3372	3357	3347	3415	3287	3442
	3519	3436	3395	3536	3485	3393	3414	3365	3428	3437	3533
	3544	3518	3445	3540	3492	3452	3510	3507	3501	3526	3537
	3630	3536	3473	3683	3788	3496	3515	3511	3522	3531	3682
A	9.6	11.8	10.4	6.0	9.4	8.9	6.9	9.6	7.6	6.7	6.0
B	2.0	1.5	2.2	1.4	1.6	1.5	1.6	0.4	1.0	1.3	1.1
C	1.6	1.3	1.9	1.2	1.4	1.4	1.3	0.4	0.9	1.1	0.9

Table 3. Reaction product branching ratios

Temperature (K)	NH_4^+ + $[CaNCO]^+$	NH_4^+ + $[CaOCN]^+$	$[H_2NCO]^+$ + $[CaNH_2]^+$	HNCO + $[CaNH_3]^{2+}$	$[CaOCNH]^{2+}$ + NH_3	$[CaNHCO]^{2+}$ + NH_3	CaO^+ + $[H_2NCNH_2]^+$
100	1.8E-07	0.013	0.010	0.008	0.969	1.6E-13	0.000
150	2.0E-07	0.014	0.020	0.016	0.950	9.4E-13	0.000
200	2.5E-07	0.014	0.051	0.039	0.895	6.4E-12	0.000
250	3.3E-07	0.015	0.121	0.092	0.773	3.9E-11	0.000
300	5.5E-07	0.017	0.228	0.173	0.582	1.9E-10	0.000
350	1.0E-06	0.020	0.338	0.257	0.386	6.8E-10	0.000
400	1.9E-06	0.026	0.418	0.318	0.239	1.8E-09	0.000
450	3.3E-06	0.034	0.465	0.354	0.147	3.9E-09	0.000
500	5.1E-06	0.042	0.491	0.373	0.093	7.3E-09	0.000

Graphical Abstract

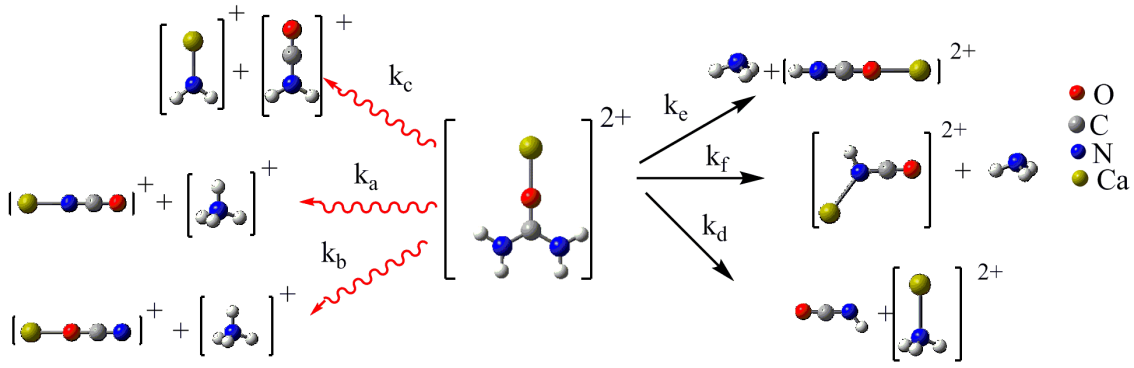

Statistical kinetic theory calculations on the reaction of Ca^{2+} with urea permit to discriminate between processes in which a neutral is lost from coulomb explosions. The kinetically preferred products are NH_3 + $[CaOCNH]^{2+}$, which are the fifth products in order of stability, whereas the most stable ones, NH_4^+ + $[CaOCN]^+$ and NH_4^+ + $[CaNCO]^+$, appear only in residual quantities..